

TARGETING A HELIOCENTRIC ORBIT COMBINING LOW-THRUST PROPULSION AND GRAVITY ASSIST MANOEUVRES

Massimiliano VASILE
Franco BERNELLI-ZAZZERA
Michelle LAVAGNA

*Dipartimento di Ingegneria Aerospaziale, Politecnico di Milano
Via La Masa 34, 20158, Milano, Italy
Vasile@aero.polimi.it*

ABSTRACT – *In this paper a direct method based on a transcription by Finite Elements in Time has been used to design optimal trajectories aiming to reach a high inclined low-perihelion orbit about the Sun, exploiting a combination of gravity assist maneuvers and low-thrust propulsion. A multiphase parametric approach has been used to introduce swing-bys among thrust and coast arcs. Gravity maneuvers are at first modeled with a link-conic approximation and then introduced through a full three-dimensional propagation including perturbations by the Sun. Finally a meaningful test case is presented to illustrate the effectiveness of the proposed approach .*

KEYWORDS: trajectory optimization and design, direct methods, finite elements in time, gravity assist maneuvers.

INTRODUCTION

Although several missions have already been flown toward the Sun, fundamental questions remain unanswered regarding our closest star. Answers could be obtained bringing instruments to yet unexplored regions of the heliosphere. This means reaching a distance from the Sun of few tens of solar radii (40-50 solar radii), possibly viewing the Sun directly from out of the ecliptic. Bringing a spacecraft to a heliocentric orbit with such a combination of low perihelion and out-of-ecliptic inclination requires a considerable amount of Δv . Using chemical propulsion, such a mission would be too expensive without resorting to multiple swing-bys of one or more planets. A solution could be to use high specific impulse units like ion or plasma drives but, even with this kind of propulsion system, the overall operating time would be excessive for state of the art engines. On the other hand, combining gravity assist maneuvers and low-thrust propulsion[1] could lead to a feasible mission in terms of transfer time propellant consumption and operating time of the engines. While swing-bys can be used to reduce the requirements in terms of Δv , low-thrust propulsion allows to shape trajectories arcs between two subsequent encounters in order to meet the best incoming conditions for a swing-by.

From a mission analysis point of view this translates into a general trajectory design and optimization problem[2]. The major difficulty consists in combining thrust arcs, which have a typical bang-bang switching structure for a minimum mass problem, with gravity maneuvers, in particular if the latter have to be introduced with an accurate fully three dimensional propagation of the hyperbolae. Furthermore, an

additional difficulty is represented by the requirement of reaching both a low perihelion and a high inclination heliocentric orbit at the same time. This means exploiting at best both the use of low-thrust propulsion and an optimal combination of swing-bys.

In this paper a direct optimization technique based on a direct transcription by Finite Elements in Time (DFET) [3] has been used to design an optimal trajectory combining low-thrust and gravity assist maneuvers leading a spacecraft to the injection into the desired heliocentric orbit. The DFET approach allows a multiphase treatment of the problem: transfer arcs between two planets and swing-bys trajectories are treated as separate phases characterized by their own reference frame and dynamic model and then assembled together to form a unique non-linear programming (NLP) problem. In addition parameters characterizing the dynamics of each phase can be included in the NLP set of variables leading to a parametric trajectory optimization.

Gravity assist maneuvers are, at first, modeled with a simple link-conic approximation, treating the periapsis altitude as parameter to be optimized, and then introduced through a three dimensional propagation of the swing-by hyperbola including 3rd body perturbations due to the Sun. Hyperbolas are propagated backward and forward from the periapsis and linked at the sphere of influence with, respectively, the incoming and outgoing trajectories. Part or all of the orbital parameters of the hyperbolas are then optimized as part of the NLP set. The simple link-conic model is quite robust and allows a fast search for an optimal combination of swing-bys. From this solution a good guess for the values of the orbital parameters of the swing-by hyperbolas can be computed and inserted in the next, more accurate, optimization.

In order to make the design process more realistic and to study the consequences of a variable thrust, the dependency of the thrust modulus on the power provided by the solar arrays is taken into account modeling accurately the behavior of the solar panels as a function of the distance from the Sun. The major effect modeled is temperature degradation, therefore the solar panels are progressively inclined with respect to the Sun in order to maintain a constant temperature.

A set of special boundary conditions is then introduced in order to target special final orbits characterized by a very low perihelion and resonant with the motion of Venus. Resonance is exploited in order to change inclination with subsequent encounters with Venus. It should be noted that resonance is not forced a priori but the DFET approach, adjusting the orbital parameters of the trajectory and the date of the encounters, in order to minimize mass consumption, leads naturally to a sequence of resonant orbits. If this is not the case, quasi-resonant orbit, characterized by a small correction using low-thrust, are allowed.

Minimum mass problem is presented targeting both a low perihelion orbit and a high inclination orbit. In the latter case, final inclination is treated either as a final constraint or as an additional objective function, which must be maximized, leading to a multiobjective optimization problem. A meaningful examples is shown demonstrating the effectiveness of the proposed approach.

PROBLEM FORMULATION

The problem is formulated in two different ways of increasing complexity. First as a reduced two body problem, with the Sun as primary and the swing-bys treated as singular events, instantaneous and with no variation in position. Then as a full three dimensional problem with swing-bys treated as actual three dimensional trajectories in space and time including perturbations. The former solution is used to provide a first guess to the latter.

The date of the encounter, as the position, are completely free as the departure date from the Earth and the injection into the final orbit. The only piece of information that must be provided is the number and name of celestial bodies used for the gravity manoeuvres. The sequence and type of celestial bodies employed distinguishes each different strategy to reach target orbit. Although guessing the swing-bys bodies could be regarded as a limitation, from a mission design point of view, it allows the analyst to design each swing-by in the most appropriate way, inserting even special conditions (e.g. coast arcs, before each encounter, required for navigation), since the early design stages.

In order to take into account swing-bys, the trajectory has been split into several phases, each phase corresponding to a trajectory arc connecting two planets. On each phase a particular collocation technique based on Finite Elements in Time has been used to transcribe differential equations, governing the dynamics of the spacecraft, into a set of algebraic nonlinear equations and to parameterise controls. When treating swing-bys as full three dimensional trajectories a local reference frame is taken to describe the gravity assist manoeuvres. Incoming conditions, at the sphere of influence, represent final conditions for the phase preceding the swing-by and outgoing conditions, at the sphere of influence, represent initial conditions for the subsequent phase. Within the sphere of influence hyperbola are propagated backward and forward in time from the pericenter in a local reference frame taking into account perturbations from the Sun. In this way collocation and multiple shooting are combined in a unique approach reducing the number of collocation points required but retaining robustness.

All the phases are then assembled together, forming a single NLP problem. Each phase is linked to the preceding one and to the following one by the appropriate set of boundary conditions computed by the relative swing-by trajectory. The resulting nonlinear programming problem (NLP) is highly sparse and has been solved efficiently by the sparse sequential programming algorithm SNOPT[4].

In the following paragraphs the dynamic model used to describe the trajectory between two encounters and the two different swing-by models employed are presented.

Dynamics

A spacecraft is modeled as a point mass subject to the gravity attraction of the Sun and to the thrust provided by one or more low-thrust engines. The motion of the spacecraft is described in the J2000 reference frame centered in the Sun (Figure1). The three components of the thrust vector \mathbf{u} represent the control:

$$\begin{aligned}\dot{\mathbf{r}} &= \mathbf{v} \\ \dot{\mathbf{v}} &= \nabla U(\mathbf{r}) + \frac{\mathbf{u}}{m_D + m_p} \\ \dot{m}_p &= -\frac{|\mathbf{u}|}{I_{sp}g_0}\end{aligned}\tag{1}$$

where the gravity potential of the Sun is a function of the position vector \mathbf{r} :

$$\begin{aligned}U(\mathbf{r}) &= \frac{\mu}{|\mathbf{r}|} \\ \mathbf{r} &= \{r_x, r_y, r_z\}^T\end{aligned}\tag{2}$$

The state and the control vectors are then defined as follows:

$$\begin{aligned}\mathbf{x} &= \{r_x, r_y, r_z, v_x, v_y, v_z, m_p\}^T; \\ \mathbf{u} &= \{u_x, u_y, u_z\}^T\end{aligned}\tag{3}$$

The mass of the spacecraft is divided into propellant mass m_p and dry mass m_D . An upper bound T_{max} and a lower bound T_{min} was put on the thrust magnitude:

$$T_{min} \leq u = \sqrt{u_x^2 + u_y^2 + u_z^2} \leq T_{max}\tag{4}$$

The upper bound is the maximum level of thrust provided by the selected low-thrust engine, the lower was taken 1×10^{-4} times T_{max} to avoid singularities in the Hessian matrix when minimum mass problems are solved. I_{sp} is the specific impulse of the engine and g_0 the gravity constant on Earth surface. The control vector \mathbf{u} can be decomposed in a local reference frame centered in the spacecraft into a tangential component u_v aligned with the velocity vector, a normal component u_n , normal to the trajectory and a bi-normal component u_h , normal to the orbital plane. In this reference frame the elevation angle ϕ is defined

as the angle between the control vector \mathbf{u} and the plane tangential to the trajectory containing \mathbf{u}_v and \mathbf{u}_h , while the azimuth angle α is defined as the angle between the projection of the control vector in the tangent plane and the velocity vector \mathbf{v} (see Fig. 1).

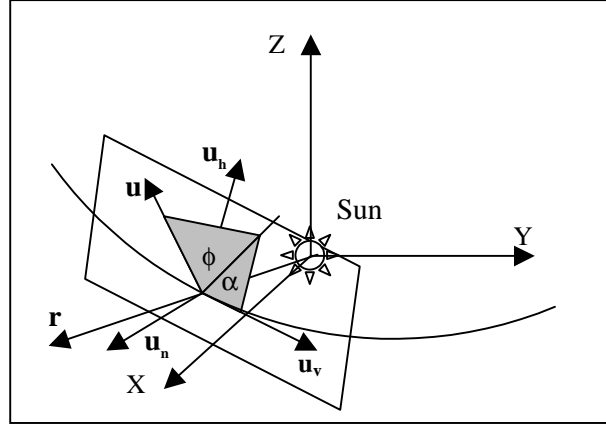


Fig. 1. Inertial reference frame centred in the Sun: the xy plane is the ecliptic plane and x axis points toward the 2000 mean vernal equinox.

Swing-by

The simplest way to model a gravity assist maneuver is to resort to link-conic approximation: the sphere of influence of a planet is assumed to have zero radius and the gravity maneuver is considered instantaneous. Therefore the instantaneous position vector is not affected by the swing-by:

$$\mathbf{r}_i = \mathbf{r}_o = \mathbf{r}_p \quad (5)$$

where \mathbf{r}_i is the incoming heliocentric position, \mathbf{r}_o is the outgoing heliocentric position vector and \mathbf{r}_p is the planet position vector, all taken at the epoch of the encounter. For an ideal hyperbolic orbit, not subject to perturbations or Δv maneuvers, the modulus of the incoming relative velocity must be equal to the modulus of the outgoing relative velocity:

$$\tilde{v}_i = \tilde{v}_o \quad (6)$$

Furthermore the outgoing relative velocity vector is rotated, due to gravity, of an angle β with respect to the incoming velocity vector and therefore the following relation must hold:

$$\tilde{\mathbf{v}}_o^T \tilde{\mathbf{v}}_i = -\cos(2\beta) \tilde{v}_i^2 \quad (7)$$

where the angle of rotation of the velocity is defined as:

$$\beta = a \cos \left(\frac{\mu}{\tilde{v}_i^2 \tilde{r}_p + \mu} \right) \quad (8)$$

All quantities with a tilde are relative to the swing-by planet and \tilde{r}_p is the periapsis radius of the swing-by hyperbola.

Numerical Propagation

After a solution has been obtained with the link-conic model, a second solution is computed substituting the simple link-conic approximation with a fully 3d numerical propagation of the swing-by hyperbolas. Each swing-by is treated as a new phase which has to be linked to the incoming part of the trajectory and to the outgoing part of the trajectory at the sphere of influence. Swing-bys are not propelled and therefore there is no need to introduce a control on the thrust vector along the swing-by hyperbola. Thus two reference frames are used and two dynamical

models: the first one is a heliocentric reference frame and the spacecraft is subject to the gravity attraction of the Sun and to the thrust of the SEP engine, the second is centred into the swing-by planet and the spacecraft is subject to the gravity attraction of the swing-by planet and to third body perturbations coming from the Sun. Thus the dynamics of the spacecraft within the sphere of influence is governed by the following differential equation:

$$\frac{d\tilde{\mathbf{x}}}{dt} = \tilde{\mathbf{F}}(\tilde{\mathbf{x}}, t) = \begin{cases} \tilde{\mathbf{v}} \\ -\frac{\mu_p}{\tilde{r}^3} \tilde{\mathbf{r}} - \mu_s \left(\frac{\mathbf{d}}{d^3} + \frac{\mathbf{r}_s}{r_s^3} \right) \end{cases} \quad (9)$$

where \mathbf{d} is the spacecraft-Sun vector and \mathbf{r}_s is the position vector of the Sun in the planetocentric reference frame. In order to increase robustness, orbital parameters for each hyperbola are not derived from incoming conditions but are included into the set of NLP parameters and then optimized. Hyperbolas are propagated backward in time from the pericenter up to the sphere of influence, where they are linked to the incoming trajectory, and forward in time up to the sphere of influence, linked to the outgoing trajectory. The value of the orbital parameters are then optimized in order to satisfy matching conditions on the sphere of influence. A first guess value for the parameter is obtained from the previous solution, the semimajor axis and the eccentricity can be easily derived from the incoming velocity modulus and from the pericenter radius:

$$a = -\frac{\mu}{\tilde{v}_i^2}; \quad e = 1 - \frac{\tilde{r}_p}{a} \quad (10)$$

The incoming and the outgoing velocity vectors must lie both in the orbital plane and therefore:

$$\begin{aligned} \mathbf{h} &= \tilde{\mathbf{v}}_i \wedge \tilde{\mathbf{v}}_o; \quad \mathbf{N} = [-h_y/h, h_x/h]^T \\ i &= a \cos \frac{h_z}{h}; \quad \Omega = a \tan \frac{h_x}{-h_y} \end{aligned} \quad (11)$$

the apsidal line $[b_x, b_y, b_z]$ must bisect the angle between the incoming and the opposite of the outgoing vector and must lie in the orbital plane, therefore the following linear system must hold:

$$\begin{bmatrix} h_x & h_y & h_z \\ \tilde{v}_x^i & \tilde{v}_y^i & \tilde{v}_z^i \\ \tilde{v}_x^o & \tilde{v}_y^o & \tilde{v}_z^o \end{bmatrix} \begin{bmatrix} b_x \\ b_y \\ b_z \end{bmatrix} = \begin{bmatrix} 0 \\ \cos \beta \\ -\cos \beta \end{bmatrix} \quad (12)$$

The three components of the apsidal axis are obtained solving the previous linear problem while the anomaly of the pericenter can be computed as the angular distance between the apsidal line and the line of the nodes:

$$\omega = a \cos \frac{\mathbf{b} \cdot \mathbf{N}}{\|\mathbf{b}\| \|\mathbf{N}\|} \quad (13)$$

In addition to the five orbital parameters, for each hyperbola the time spent within the sphere of influence is derived from the semimajor axis and the eccentricity:

$$\cosh H = \frac{1}{e} \left(1 - \frac{\tilde{r}_i}{a} \right) \quad (14)$$

$$\Delta t = (e \sinh H - H) \sqrt{\frac{a^3}{\mu}} \quad (15)$$

This value is used to integrate backward in time the state vector computed at the pericenter of the hyperbola up to the sphere of influence and forward in time the same state vector up to the sphere of influence. The state vector at the pericenter of the hyperbola is computed from the orbital parameters:

$$[\tilde{\mathbf{r}}_p, \tilde{\mathbf{v}}_p]^T = f(a, e, i, \omega, \Omega, 0) \quad (16)$$

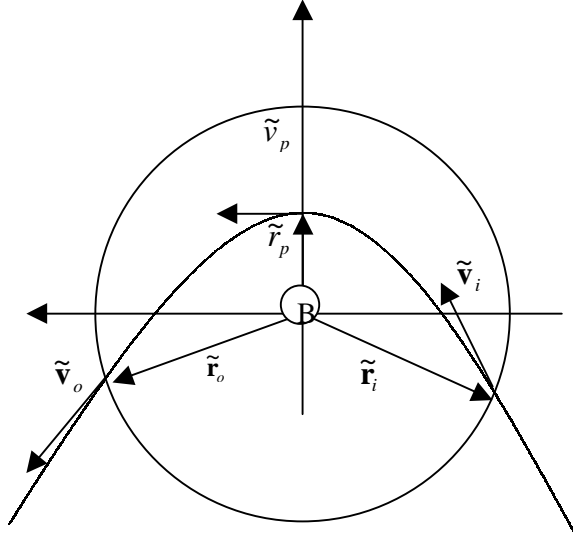


Fig. 2. Swing-by model and reference frame

Therefore at the sphere of influence of a body B, with state vector $[\mathbf{r}_B, \mathbf{v}_B]^T$, the following set of matching constraints must be satisfied:

$$\begin{aligned} \tilde{\mathbf{v}}_i &= \mathbf{v}_i - \mathbf{v}_B(t - \Delta t) \\ \tilde{\mathbf{r}}_i &= \mathbf{r}_i - \mathbf{r}_B(t - \Delta t) \end{aligned} \quad (17)$$

$$\begin{aligned} \tilde{\mathbf{v}}_o &= \mathbf{v}_o - \mathbf{v}_B(t + \Delta t) \\ \tilde{\mathbf{r}}_o &= \mathbf{r}_o - \mathbf{r}_B(t + \Delta t) \end{aligned} \quad (18)$$

where incoming and outgoing relative position and velocity vectors are obtained integrating respectively from t to $t - \Delta t$ and from t to $t + \Delta t$ the differential equations:

$$\begin{aligned} \tilde{\mathbf{x}}_i &= \tilde{\mathbf{x}}_p + \int_t^{t-\Delta t} \tilde{\mathbf{F}}(\tilde{\mathbf{x}}, t) dt \\ \tilde{\mathbf{x}}_o &= \tilde{\mathbf{x}}_p + \int_t^{t+\Delta t} \tilde{\mathbf{F}}(\tilde{\mathbf{x}}, t) dt \end{aligned} \quad (19)$$

Figure 2 reports a sketch of the model adopted for swing-bys.

Thrust Model

The thrust provided by the engine is determined taking into account the specific thrust F_{sp} the effective input power P_{in} provided by the power system and an efficiency coefficient η_e :

$$F_{\max} = \eta_e P_{in} F_{sp} \quad (20)$$

The effective input power is given by the effective power produced by the solar arrays minus the power required by the spacecraft P_{ss} :

$$P_{in}^* = P_{eff} - P_{ss} \quad (21)$$

In order to take into account the degradation of the solar arrays due to temperature and the reduced power due to the increasing distance from the sun, the power provided by the solar arrays during the transfer trajectory is here expressed as:

$$P_{eff} = \eta_s \frac{P_{1AU}}{R_s^2} [1 - C_T(T_s - T_0)] \cos \alpha \quad (22)$$

where P_{1AU} is the power at one Astronomical Unit, T_s is the temperature of solar arrays, R_s is the distance from the Sun, T_0 the reference temperature, C_T is the temperature coefficient which express the reduced

performance of the panel with temperature increase, η_s is a coefficient to account for all other degradations sources and α is the solar array sun aspect angle, i.e. the angle between the normal to the cell surface and the sun direction. The steady state surface temperature of the solar panels is here taken as function of the distance from the sun:

$$T_s = \left[\frac{S_0 \alpha_s \cos \alpha}{R_s^2 \sigma \kappa \epsilon} \right]^{0.25} \quad (23)$$

where S_0 is the solar constant at 1 AU, σ is the Stefan-Boltzmann constant, α_s is the surface absorptivity in the solar spectrum and ϵ is the surface emissivity in the infrared spectrum, κ is a coefficient which takes into account the surface area radiating in the infrared spectrum, with respect to the one that receives the solar input. A maximum power that can be handled by the PPU is assumed to represent the upper limit for the engine thrust.

$$P_m = \min(P_m^*, P_{\max}) \quad (24)$$

The required power is dimensioning for the design of the solar arrays and power system and therefore it provides estimation for the overall dry mass of the spacecraft. Power supply characteristics are summarized in Table 1.

Table 1. Power system characteristics

Parameter	Value
η_c	0.9
η_s	1
P_{IAU}	14.5 kW
C_T	$3 \cdot 10^{-4} \text{ K}^{-1}$
T_0	290 K
κ	1.3
ϵ	.86
α	.86
T_{max}	423 K
P_{max}	15 kW
P_{SS}	300 W

Resonant Constraint

For some applications the Δv provided by a single swing-by is not enough to increase or decrease sufficiently a given orbital parameter. Repeated encounters with the same celestial body performing several swing-bys sequentially distributed in time leads to increase or decrease progressively one or more orbital parameters, therefore for some application it is required to insert a spacecraft into an orbit resonant with the motion of a planet. Incoming conditions must be computed at the end of an integer number of revolutions after each swing-by. Parameterise each revolutions using collocation is useless unless perturbations are considered and not efficient.

Therefore a special final constraint can be introduced to compute incoming conditions collocation just a single revolution. If no perturbations are considered final state at the end of the first revolution, after each swing-by, can be projected forward in time for a period $n-1$ times the period of the resonant orbit, where n is the number of revolutions required to encounter again the planet. The celestial body is therefore located at the epoch of the expected encounter and the final position vector of the first revolution is constrained to be equal to the position vector of the planet, in case of link-conic approximation, or to the sphere of influence of the planet in case of three dimensional propagation of the hyperbola. The semimajor axis is of course a free parameter and is computed from the outgoing conditions, therefore even each time of each subsequent encounter results to be a free parameter.

OPTIMISATION APPROACH

A general trajectory design problem can be decomposed in M phases, each one characterized by a time domain D^j , with $j=1, \dots, M$, a set of m dynamic variables \mathbf{x} , a set of n control variables \mathbf{u} and a set of l parameters \mathbf{p} . Furthermore, each phase j may have an objective function

$$J^j = \phi^j(\mathbf{x}_0^b, \mathbf{x}_f^b, t_f, \mathbf{p}) + \int_{t_i}^{t_f} L^j(\mathbf{x}, \mathbf{u}, \mathbf{p}) dt \quad (25)$$

a set of dynamic equations

$$\dot{\mathbf{x}} - \mathbf{F}^j(\mathbf{x}, \mathbf{u}, \mathbf{p}, t) = 0 \quad (26)$$

a set of algebraic constraints on states and controls

$$\mathbf{G}^j(\mathbf{x}, \mathbf{u}, \mathbf{p}, t) \geq \mathbf{0} \quad (27)$$

and a set of boundary constraints

$$\psi^j(\mathbf{x}_0^b, \mathbf{x}_f^b, \mathbf{p}, t) \Big|_{t_0}^{t_f} \geq 0 \quad (28)$$

Among boundary constraints a set of inter-phase link constraints exist that are used to assemble all phases together

$$\psi^j(\mathbf{x}_j^b, \mathbf{x}_{j-1}^b, \mathbf{p}, t) \geq 0 \quad (29)$$

The time domain $D(t_o, t_p) \subset \mathcal{R}$ relative to each phase j can be further decomposed into N finite time elements $D^j = \bigcup_{i=1}^N D_i^j(t_{i-1}, t_i)$ and, on each time element D_i^j , states and controls $[\mathbf{x}, \mathbf{u}]$ can be parameterized as follows:

$$\begin{Bmatrix} \mathbf{x} \\ \mathbf{u} \end{Bmatrix} = \sum_{s=1}^p f_s(t) \begin{Bmatrix} \mathbf{x}_s \\ \mathbf{u}_s \end{Bmatrix} \quad (30)$$

where the basis functions f_s are chosen within the space of polynomials of order $p-1$:

$$f_s \in P^{p-1}(D_i^j) \quad (31)$$

Therefore in general a finite element is defined by a sub-domain D_i^j , and by a sub-set of parameters $[\mathbf{x}_s, \mathbf{u}_s, \mathbf{p}]$. A group of finite elements forms a phase and a group of phases forms the original optimization problem. Notice that additional parameters \mathbf{p} may occur in all constraint equations depending on their function in the optimization problem. Furthermore it should be noticed that each phase can be grouped in sequence or in parallel with the other phases depending on its time domain and on the inter-phase link constraints that pass information among phases. Thus two phases can share the same time domain but have different parameterizations.

Now taking a general phase, in order to integrate differential constraints (26), on each finite element i , differential equations are transcribed into a weighted residual form considering boundary conditions of the weak type:

$$\int_{t_i}^{t_{i+1}} \{ \dot{\mathbf{w}}^T \mathbf{x} + \mathbf{w}^T \mathbf{F}^j \} dt - \mathbf{w}_{i+1}^T \mathbf{x}_{i+1}^b + \mathbf{w}_i^T \mathbf{x}_i^b = 0 \quad i = 1, \dots, N-1 \quad (32)$$

where $\mathbf{w}(t)$ are generalized weight (or test) functions defined as:

$$\mathbf{w} = \sum_{s=1}^{p+1} g_s(t) \mathbf{w}_s \quad (33)$$

where g_s are taken within the space of polynomials of order p :

$$g_s \in P^p(D_i^j) \quad (34)$$

Now the problem is to find the vector $\mathbf{x}_s \in \mathfrak{R}^{p^*m}$, the vector $\mathbf{u}_s \in \mathfrak{R}^{p^*n}$, the vector $\mathbf{p} \in \mathfrak{R}^l$ and \mathbf{x}_f^b and $\mathbf{x}_0^b \in \mathfrak{R}^m$ that satisfy variational equation (32) along with algebraic and boundary constraints:

$$\mathbf{G}^j(\mathbf{x}, \mathbf{u}, \mathbf{p}, t) \geq 0 \quad (35)$$

$$\psi^j(\mathbf{x}_0^b, \mathbf{x}_f^b, \mathbf{p}, t) \Big|_{t_0}^{t_f} = 0 \quad (36)$$

where quantities \mathbf{x}_s and \mathbf{u}_s are called internal node values, while \mathbf{x}_f^b , \mathbf{x}_0^b are called boundary values. Notice that generally the order p of the polynomials can be different for states and controls. In a more general way the domain D^j could be decomposed as a union of smooth images of the reference time interval $[-1,1]$ where a reference parameter τ is defined as:

$$\tau = 2 \frac{t - t_{i-1/2}}{t_i - t_{i-1}} = 2 \frac{t - t_{i-1/2}}{\Delta t_i} \quad (37)$$

Polynomials f_s and g_s are constructed using Lagrangian interpolants associated with internal Gauss-type nodes. Generally speaking if $\{\xi_s^j\}_{s=1}^p$ are the set of Gauss points on the reference interval $[-1,1]$, $f_s(\tau)$ will be the Lagrangian interpolating polynomial vanishing at all Gauss points except at ξ_s^j where it equals one. Each integral of the continuous forms (25) and (32) is then replaced by a q -points Gauss quadrature sum, where q is taken equal to p . Therefore the objective function (25) becomes a sum of N Gauss quadrature formulas:

$$J^j = \phi^j(\mathbf{x}_0^b, \mathbf{x}_f^b, t_f) + \sum_{i=1}^N \sum_{k=1}^q \sigma_k L^j_k \frac{\Delta t_i}{2} \quad (38)$$

while integral (32) is split into N integrals of the form:

$$\sum_{k=1}^q \sigma_k \left[\dot{\mathbf{w}}_k(\tau_k)^T \mathbf{x}(\tau_k) + \mathbf{w}_k(\tau_k)^T \mathbf{F}^j_k \frac{\Delta t_i}{2} \right] - \mathbf{w}_{p+1}^T \mathbf{x}_{p+1}^b + \mathbf{w}_1^T \mathbf{x}_1^b = 0 \quad i=1, \dots, N-1 \quad (39)$$

where σ_k are Gauss weights and parameters \mathbf{x}_{i-1}^b and \mathbf{x}_i^b are boundary values at the beginning and at the end of each element. For sake of simplicity, the following notation has been introduced:

$$L^j_k = L^j(\mathbf{x}_s f_s(\tau_k), \mathbf{u}_s f_s(\tau_k), \mathbf{p}, \tau_k); \quad \mathbf{F}^j_k = \mathbf{F}^j(\mathbf{x}_s f_s(\tau_k), \mathbf{u}_s f_s(\tau_k), \mathbf{p}, \tau_k) \quad (40)$$

Here controls are parameterized using the same set of points used for integration while states are always collocated on Gauss-Lobatto nodes. Numerical quadrature of the integral Eq. (32) and integral (25) can be then performed either by Gauss Lobatto rule or by Gauss-Legendre rule. The former choice of quadrature formulas collocates controls on the same set of nodes as states while the latter collocates controls on a different set. The advantage of the latter is the higher integration order which allows a lower number of collocation nodes. Whatever f_s and g_s are, the linear part of Eq. (39) can be always integrated only once before the optimization process begins. Now Eq. (39) must be satisfied for every arbitrary value of virtual quantity \mathbf{w}_k , as a consequence each element equation is developed into $p+1$ equations:

$$\sum_{k=1}^q \sigma_k \mathbf{F}^j_k \frac{\Delta t_i}{2} \begin{Bmatrix} g_1(\tau_k) \\ \vdots \\ g_{p+1}(\tau_k) \end{Bmatrix} + \begin{Bmatrix} \sum_{k=1}^q \sigma_k \dot{g}_1(\tau_k) f_1(\tau_k) & \cdots & \sum_{k=1}^q \sigma_k \dot{g}_1(\tau_k) f_p(\tau_k) \\ \vdots & \ddots & \vdots \\ \sum_{k=1}^q \sigma_k \dot{g}_{p+1}(\tau_k) f_1(\tau_k) & \cdots & \sum_{k=1}^q \sigma_k \dot{g}_{p+1}(\tau_k) f_p(\tau_k) \end{Bmatrix} \begin{Bmatrix} \mathbf{x}_1 \\ \vdots \\ \mathbf{x}_p \end{Bmatrix} = \begin{Bmatrix} -\mathbf{x}_i^b \\ 0 \\ \mathbf{x}_{i+1}^b \end{Bmatrix} \quad (41)$$

System of Eqs. (41) is written for each element, all the elements are then assembled matching the final boundary node of one element to the initial one of the next element. For continuous solution, in order to preserve the continuity of the states, at matching points, the following condition must hold:

$$\mathbf{x}_i^b = \mathbf{x}_{i+1}^b \quad i=1, \dots, N-2 \quad (42)$$

Thus all the boundary quantities (42) cancel one another except for those at the initial and final times. Algebraic constraint equation (35) can be collocated directly at Gauss nodal points:

$$\mathbf{G}^j_s(\mathbf{x}_s(\xi_s), \mathbf{u}_s(\xi_s), \mathbf{p}, \xi_s) \geq 0 \quad (43)$$

The resulting set of non-linear algebraic equations, assembling all the phases, along with discretised objective function (38) can be seen as a general non-linear programming problem (NLP) of the form:

$$\min J(\mathbf{y}) \quad (44)$$

subject to

$$\begin{aligned} \mathbf{c}(\mathbf{y}) &\geq 0 \\ \mathbf{b}_l &\leq \mathbf{y} \leq \mathbf{b}_u \end{aligned} \quad (45)$$

where, \mathbf{y} is the vector of NLP variables, $J(\mathbf{y})$ the objective function to be minimized, $\mathbf{c}(\mathbf{y})$ a vector of non-linear constraints and \mathbf{b}_l and \mathbf{b}_u respectively lower and upper bounds on NLP variables. The $N*(p+1)*n$ algebraic Eqs. (41) taken for each phase, along with system (43), represent the $\mathbf{c}(\mathbf{y})$ constraint of the nonlinear problem while $\mathbf{y}=[\mathbf{x}_s, \mathbf{u}_s, \mathbf{x}_0^b, \mathbf{x}_1^b, t_\rho, t_p, \mathbf{p}]$ the NLP variables. Notice that the present formulation is discontinuous because continuity at boundaries of each element is only weakly enforced. This means that, generally, there is a jump between the internal nodes and the boundary nodes. This allows the control, for which no continuity requirement is imposed, to be discontinuous at boundaries.

RESULTS

The proposed approach to design an optimal trajectory aiming to reach a low-perihelion high-inclined orbit has been used to find a solution for the ESA mission SOLO. The strategy, or sequence of swing-bys, used an optimized version of the one proposed by Langevin for SOLO[5] and exploits a sequence of swing-bys of Venus to increase the inclination and to reduce the altitude of perihelion. This strategy, called EVE in this paper, exploits a swing-by of the Earth to reach the first perihelion before the insertion into the resonant orbit. In the following the two strategies will be presented in more details.

EVE strategy

The aim is to inject a 1510 kg, wet mass at launch, spacecraft into a low-perihelion high-inclined orbit to observe the Sun from outside the ecliptic plane. Using just electric propulsion to increase inclination would be too expensive and prohibitive for state-of-the-art engines due to the excessive operating time. A solution to the problem would be to perform a sequence of swing-bys of one or more celestial bodies. In order to spend as much time as possible at the perihelion, the aphelion should not be too high, that is to say with an altitude lower than the orbit of the Earth. The best candidate is therefore Venus because Mercury is less massive and the Earth is too high. Therefore the spacecraft is injected into a transfer trajectory that, after an initial swing-by of Venus, leads to an encounter with Earth that reduces the perihelion down to 0.24 AU. After two revolutions around the Sun the spacecraft is injected into a resonant orbit with a period 2/3 of the period of Venus. Every three complete revolutions, therefore, the spacecraft performs a swing-by with Venus, increasing progressively its inclination.

It should be noted that the altitude of the last perihelion before the injection into the resonant orbit plays a fundamental role. In fact, propellant consumption is greatly influenced by this parameter, furthermore an high gain in inclination can be achieved reducing the demands in terms of perihelion altitude. For navigation reasons before each encounter a coast arc of about 30 days should be inserted to allow a good

orbit determination especially before each swing-by. This is realized introducing a phase where the control magnitude is forced to be zero.

Once the probe has reached the resonant orbit the resonant constraint is inserted and a phase is inserted each time an increase in inclination is desired. To cope with SOLO mission three phases, with three resonant constraints (corresponding to nine revolutions around the Sun) has been inserted reaching an inclination of 32° .

The objective function to be minimized is the total propellant mass to reach the final orbit, departure is constrained to be on the sphere of influence of the Earth with an asymptotic velocity of about 2.5 km/s. The maximum thrust provided by the engine is of 0.3 N, quite low compared to the initial mass, while the Isp is 2100 s. It should be noted that the actual thrust level depends greatly on the position with respect to the Sun and is computed according to the model presented above. Due to the close approach to the Sun the temperature of the solar panel increase meaningfully and, therefore, the angle between the normal to the solar arrays and the Sun-spacecraft direction is progressively increased.

The resulting trajectory is represented in Figs. 3,4 and 5, the solution obtained with DFET has been propagated forward in time using a variable order, variable step extrapolation integrator to verify the quality of the solution. The DFET solution is propagated in a heliocentric reference frame with an n-body gravity model (i.e. including actual gravity of each planet). The solid line represents thrust arcs while the dashed line represents coast arcs. As can be clearly seen the imposed period of 30 days before each encounter is satisfied. A circle marker represent the departure from the Earth while stars represent swing-bys and two star marker represent respectively the entry into the sphere of influence end the exit point from the sphere of influence for each swing-by. Each swing by is fully numerical, the result obtained after propagation is represented in Fig.14 and 15 where a close up of the semimajor axis is represented for the first two swing-bys showing the accuracy of the DFET solution. In fact the error at the sphere of influence where the propagated hyperbola are linked to the transfer arcs is less than $1e-3$.

Orbital parameters are represented in Figs. from 6 to 10, in particular it is worth noticing Fig. 8 where the effect of the resonant constraint is evident on the behavior of then inclination. As can be seen the end of each resonant orbit is projected forward in time where the next swing-by occurs and increases the inclination.

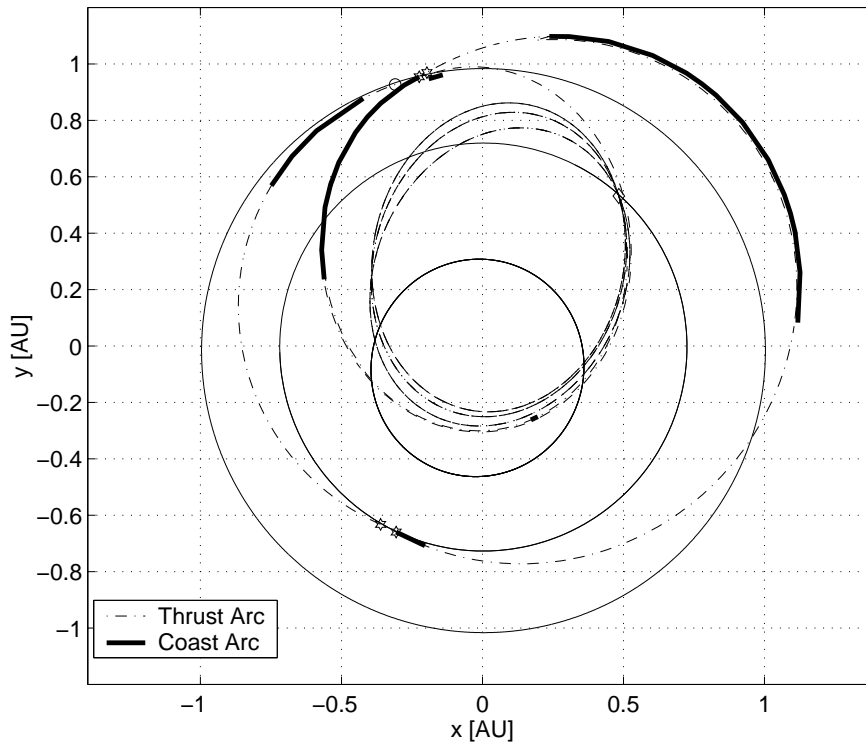


Fig. 3. Trajectory in the ecliptic plane for the case with EVE strategy

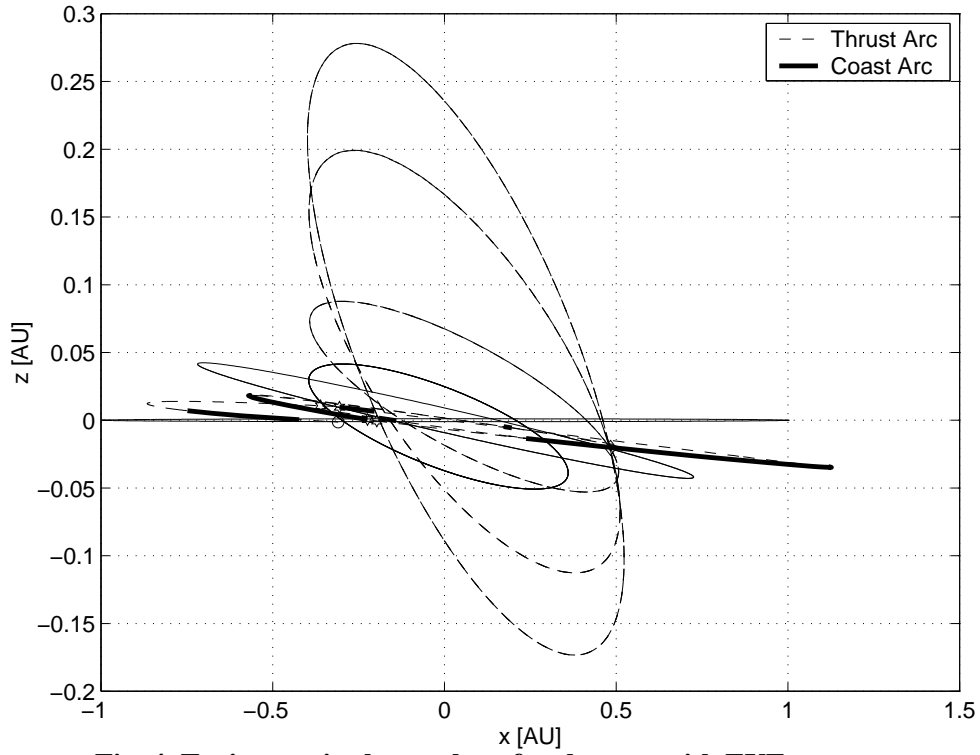


Fig. 4. Trajectory in the xz plane for the case with EVE strategy

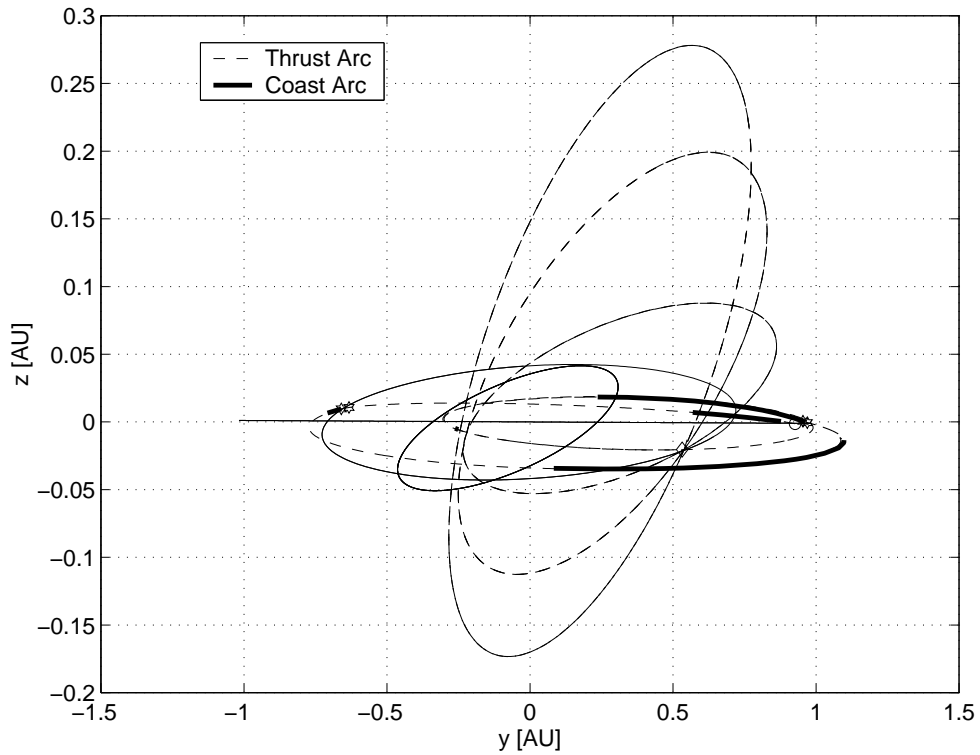


Fig. 5. Trajectory in the yz plane for the case with EVE strategy

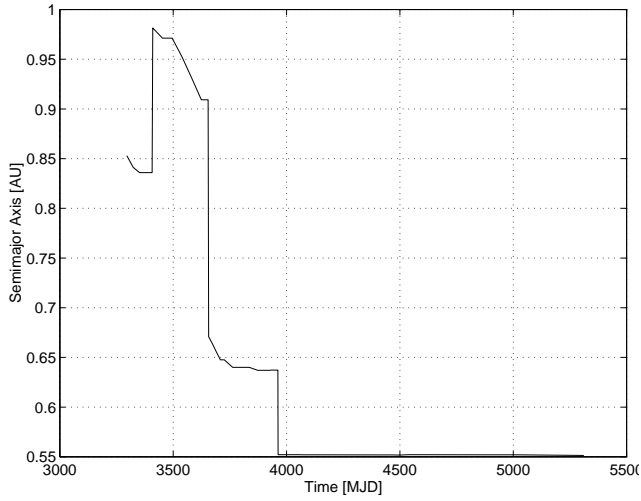


Fig. 6. Semimajor Axis

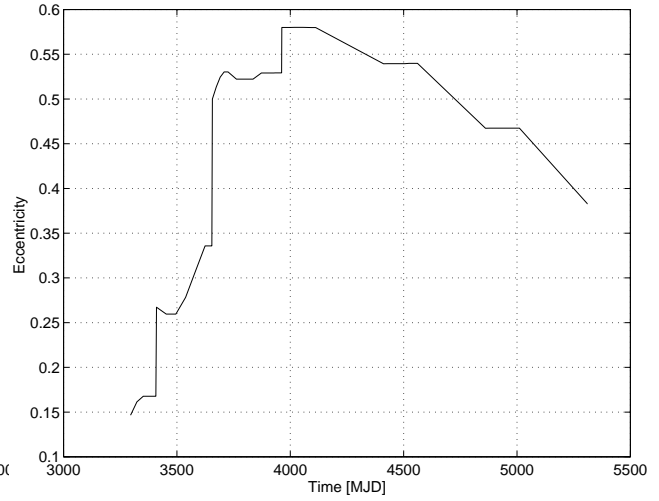


Fig. 7. Eccentricity

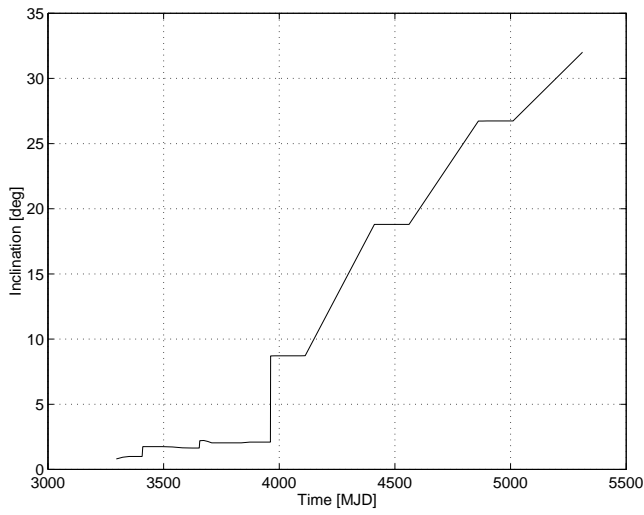


Fig. 8. Inclination

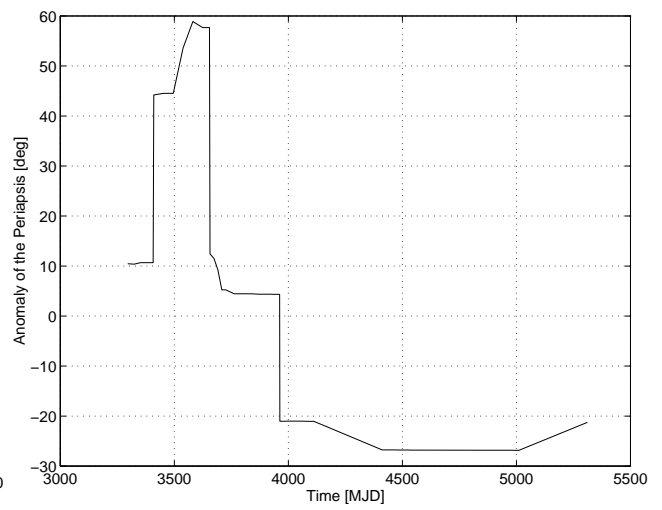


Fig. 9. Argument of the Ascending Node

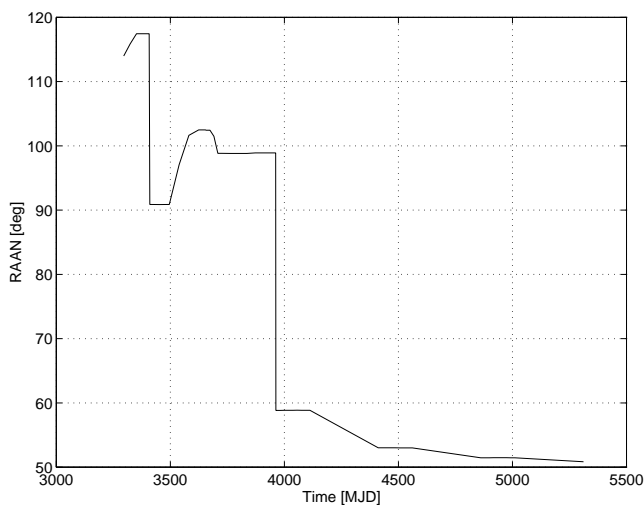


Fig. 10. Argument of the Perihelion

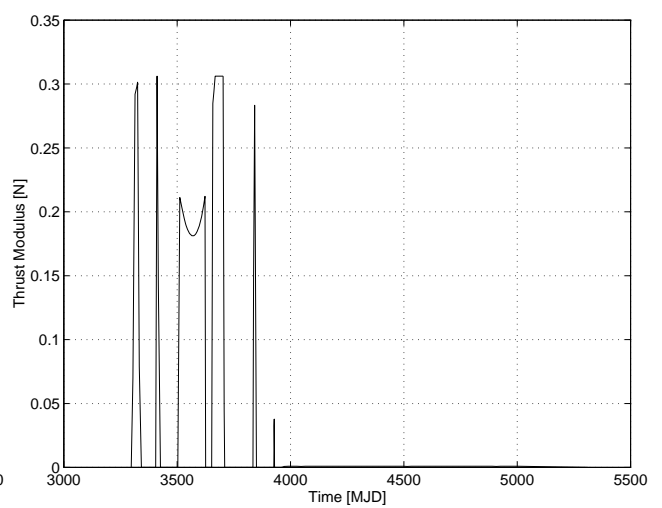


Fig. 11. Thrust magnitude as a function of time

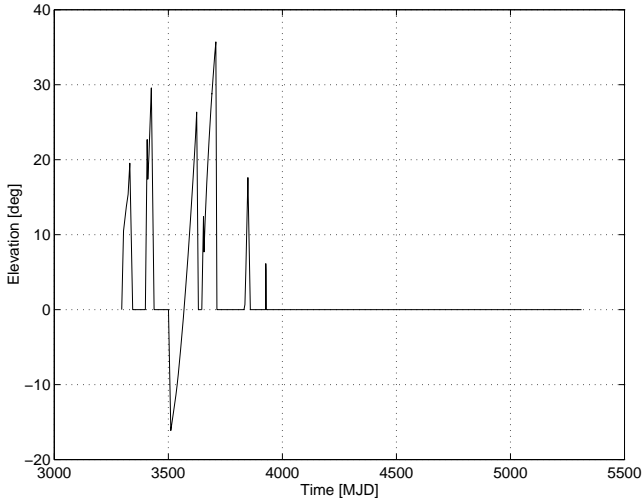


Fig. 12. Thrust Elevation Angle

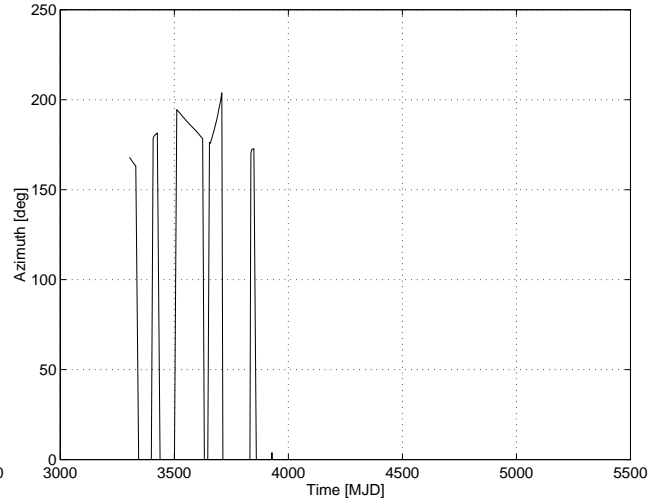


Fig. 13. Thrust Azimuth Angle

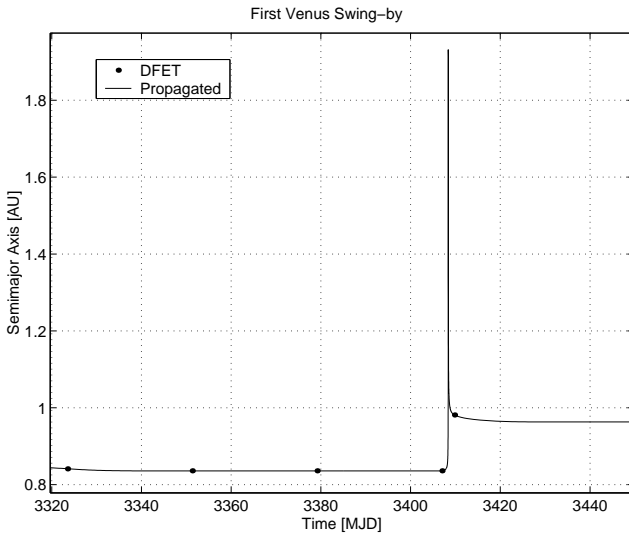


Fig. 14. First Venus Swing-by

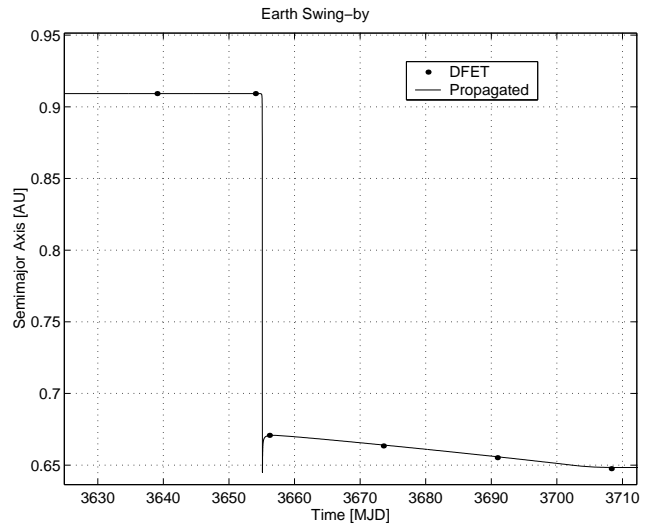


Fig. 15. Earth Swing-by

Table 2 Transfer Trajectory: summarizing table

DATA	SOLO		IMPROVED EVE	
v_{∞}	2.51 km/s		2.51 km/s	
Max Thrust	0.3(power dependent)		0.3 (power dependent)	
Isp	2100 s		2100 s	
Launch Date	03 Jan 2009		08 Jan 2009	
Initial Mass	1510 kg		1510 kg	
Final Mass	1197.7 kg		1303.9 kg	
Target Inclination	31.7°		32°	
Arrival Date	13 Oct 2015		16 Jul 2014	
	Altitude	Date	Altitude	Date
Venus Swing-by	/	30 Apr 2009	1427 km	29 Apr 2009
Earth Swing-by	300 km	01 Jan 2010	398.7 km	02 Dec 2009
Venus Swing-by	300 km	06 Jul 2010	300 km	05 Nov 2010
Venus Swing-by	300 km	31 Nov 2011	300 km	29 Jan 2011
Venus Swing-by	300 km	23 Apr 2013	300 km	22 Apr 2013
Venus Swing-by	300 km	16 Jul 2014	300 km	15 Jul 2013
Venus Swing-by	300 km	10 Oct 2015	/	/

Thrust modulus with respect to time is represented in Fig. 11, showing the dependency on power provided by the solar arrays, while elevation and azimuth angles are represented respectively in Figs. 12 and 13. A comparison between SOLO solution and the improved EVE strategy presented in this paper, is reported in Table 2. As can be seen the improved solution presents quite a substantial gain in mass delivered into the final orbit with a reduced time of transfer (one swing-by less is required to reach the same final inclination). As mentioned before, this has been obtained reducing the demands in terms of perihelion in fact the lowest perihelion reached is 0.227 AU while SOLO solution reaches 0.21 AU as lowest perihelion.

CONCLUSIONS

In this paper the problem of designing an optimal transfer trajectory from the Earth to a low-perihelion high-inclined orbit about the Sun has been solved with a direct optimization approach and a transcription by Finite Elements in Time. The trajectory optimization problem is particularly complex due to the combination of low-thrust and multiple gravity assist maneuvers used to reduce the demands in terms of Δv . The problem is split into phases and for each one both states and controls are parameterized using DFET, an additional set of parameters is then included leading to a direct multiphase parametric optimization of the trajectory. Swing-bys are, at first, introduced through a simplified link-conic model for which the altitude is a parameter to be optimized then they are introduced as a full propagation of the hyperbolae. In the latter case orbital parameters of the hyperbolae are included among NLP parameters and optimized. The parametric optimization using a combination of collocation by FET and shooting is quite robust and solves efficiently and accurately the problem with a reduced set of NLP variables.

The improved solution reaches the target inclination about one year early with a gain of about 106 kg in mass just relaxing slightly the requirements in terms of perihelion altitude. In fact, no constraints either on this parameter or on the node axis have been imposed. Forcing such kind of constraints could lead to an increase in mass consumption and to a reduced gain in inclination at each encounter with Venus.

ACKNOWLEDGMENT

The authors would like to thank Dr. Guy Janin of the European Space Operation Centre (ESOC/ESA) for the data relative to SOLO trajectory.

REFERENCES

- [1] Y.Langevin. "Chemical and Solar Electric Propulsion Options for a Mercury Cornerstone Mission". IAF-99-A.2.04, *50th IAF Congress* 4-8 October 1999 Amsterdam.
- [2] Vasile M, Bernelli-Zazzera F. "Combining Low-Thrust Propulsion and Gravity Assist Manoeuvres to Reach Planet Mercury". AAS 01-459, *AAS/AIAA Astrodynamics Specialist Conference*, Quebec City, Quebec, Canada, July 30-August 2, 2001
- [3] Vasile M. "Direct Transcription by FET for Optimal Space Trajectory Design". *Internal Report DIA-SR 99-02*, Politecnico di Milano, Dipartimento di Ingegneria Aerospaziale, March 1999.
- [4] Gill P.E., Murray W., Saunders A. "User's Guide for SNOPT 5.3: A Fortran Package for Large-Scale Nonlinear Programming". Stanford University, 1998.
- [5] ESA. "Pre-Assessment Study Report: Solar Orbiter", CDF-02(A) October 1999.

